Supporting information

Ultrathin $Cu(In,Ga)Se_2$ solar cells with passivated back interface: a comparative study between Mo and In_2O_3:Sn back contacts

Yong Li[1], Guanchao Yin[2*], Ye Tu[2], Setareh Sedaghat[1], Yao Gao[1], Martina Schmid[1*]

[1]*Faculty of Physics, University of Duisburg-Essen & CENIDE, Forsthausweg 2, 47057 Duisburg, Germany*

[2]*School of Materials Science and Engineering, Wuhan University of Technology, Luoshi Road 122, 430070 Wuhan, China*

** Corresponding authors:*

Martina Schmid, E-mail: martina.schmid@uni-due.de;

Guanchao Yin, E-mail: guanchao.yin@whut.edu.cn.

Table S1. j_{abs} dependent on the SiO_2 thickness and the back contact material. **(a)** represents the structure of glass/400 nm Mo/0 or 50 nm SiO_2/500 nm CIGSe/60 nm CdS/80 nm i-ZnO/300 nm AZO and **(b)** glass/300 nm ITO/0 or 50 nm SiO_2/500 nm CIGSe/60 nm CdS/80 nm i-ZnO/300 nm AZO.

Thin films structure	SiO_2 thickness (nm)	j_{abs} (mA/cm^2)	j_{abs} gain compared to 0 nm SiO_2 (mA/cm^2)
(a)	0	25.8	-
	50	26.7	0.9
(b)	0	25.1	-
	50	25.3	0.2

To quantitatively estimate the optical absorption enhancement in the CIGSe absorber caused by the SiO_2 layer insertion, the photocurrent equivalent to absorption j_{abs} is defined as:

$$j_{abs} = \int_{350}^{1200} n(\lambda) * A(\lambda) * e * d\lambda \quad (1)$$

where $n(\lambda)$ is the number of photons at the corresponding wavelength in the solar spectrum, $A(\lambda)$ the absorption of the ultrathin CIGSe absorber, e the elementary charge and λ the wavelength. $A(\lambda)$ is extracted from RefDex [1] simulation results.

For simplicity, a planar SiO_2 layer is assumed in the simulation and the refractive index of SiO_2 is set to be constant 1.5. The wavelength range only covers 350-1200 nm.

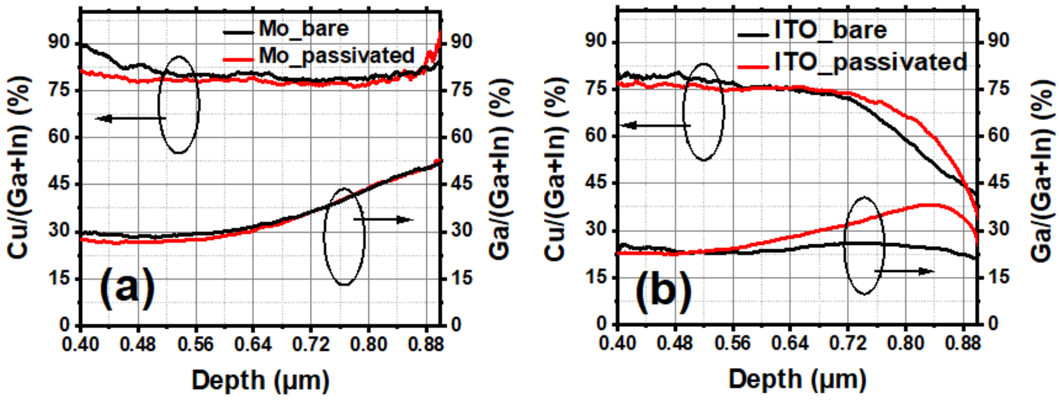

Figure S1. GD-OES (Glow discharge optical emission spectroscopy) data comparing Cu/(Ga+In) and Ga/(Ga+In) ratio depth distributions for ultrathin CIGSe solar cells without (_bare) and with (_passivated) SiO_2 point contact passivation layer on a) Mo and b) ITO back contact.

For Mo_bare and Mo_passivated, the Cu/(Ga+In) and Ga/(Ga+In) ratios are overlapping with each other. It implies that the ultrathin CIGSe absorbers on both Mo substrates have the same compositional gradient and the SiO_2 point contacts do not have a significant influence on the CIGSe element distribution. In the case of ITO_passivated, however, the Cu/(Ga+In) and Ga/(Ga+In) ratios are slightly higher than for ITO_bare. This is because the SiO_2 layer hindered the indium signal from the ITO (In_2O_3:Sn) substrate when the plasma of the GD-OES was etching down to the ITO back contact, as the etching cave is not a perfect rectangular, but a valley with curved edges. Judging from the Ga and Cu ratio on the CdS side (corresponding to the depth of 0.40 µm), and the fact that all the ultrathin CIGSe absorbers come from the same co-evaporation batch, the composition would in truth be equal for all samples.

Table S2. Experimental PV parameters of ultrathin CIGSe solar cells with different point contact ratios on different back contacts.

Back contact	Contact area ratio (%)	Etching time (min)	V_{oc} (mV)	j_{sc} (mA/cm^2)	*FF* (%)	E_{ff} (%)	Presented sample in the main manuscript
Mo	100	0	609±6.2	25.3±1.0	61.8±4.4	9.5±0.6	**Mo_bare (no SiO_2)**
	40	15	606±3.8	26.4±1.4	67.9±1.6	10.9±0.4	
	22	22	609±4.7	28.2±2.2	64.5±2.3	11.1±0.9	**Mo_passivated (22% SiO_2 coverage)**
	8	30	608±4.5	27.5±1.0	62.0±1.6	10.4±0.3	
ITO	100	0	597±3.1	26.6±1.1	59.9±3.6	9.5±0.4	**ITO_bare (no SiO_2)**
	40	15	580±4.6	26.7±1.1	58.0±2.0	9.0±0.3	
	22	22	574±6.5	26.9±1.2	58.0±1.7	9.0±0.2	**ITO_passivated (22% SiO_2 coverage)**
	8	30	466±19.9	13.3±3.6	19.6±2.3	1.2±0.5	

Table S2 summarize the PV parameters of the ultrathin CIGSe solar cells with different SiO_2 point contact ratios and different back contacts. The etching time means the O_2 plasma etching time period used to shrink the diameter of the PS spheres. On the Mo substrates, we notice that there is a small deviation from sample to sample, but it is a relatively small one, as the amplitude of the deviation is 1-2 mV in the averaged V_{oc}. Two reasons are responsible: Firstly, the steep back Ga grading in the samples (See supporting Figure S1). It repels photogenerated electrons from back contact and thus restrains the back recombination, which acts similarly to passivation. Exactly because of this, back interface passivation will bring a reduced beneficial effect on ultrathin cells with a high Ga grading. Secondly, since the absorbers were prepared at a quite low temperature (450 °C maximum), the interfacial $MoSe_x$ may not have formed well. This will decrease V_{oc} to a certain degree. Under the combined actions of these two factors, the V_{oc} remains stable after back interface passivation for ultrathin CIGSe solar cells on Mo. Compared to Mo_bare, the j_{sc} is improved for all the passivated samples to a different degree, depending on the SiO_2 coverage. This is because the recombination at the CIGSe/Mo is supressed, and the reflection from the CIGSe/SiO_2/Mo interface is enhanced. Overall, all the SiO_2 passivated solar cells on Mo show higher *Eff* than the reference samples.

On the ITO substrates, however, the V_{oc} shows a clear decreasing trend. So do *FF* and *Eff*, showing a monotonous drop. Only in j_{sc}, the solar cells with 22% and 40% contact area ratio show a tiny increase compared to the bare ITO. All the PV parameters of the 8% contact area ratio are severely diminished, because the current at the back contact is suppressed to extreme.

Table S3. Model parameters used in SCAPS for the structure of Back Contact/CIGSe/ODC/CdS/i-ZnO/AZO, whereby ODC stands for ordered-defect-compound, AZO for ZnO:Al and i-ZnO for intrinsic ZnO. For details about the definition file of this model, please contact the authors.

Layer Parameter	**Symbol (Unit)**	**Back Contact**	**CIGSe**	**ODC**	**CdS**	**i-ZnO**	**AZO**
Thickness	d (nm)	-	485	15	50	80	300
Bandgap	E_g (eV)	-	1.10	1.45	2.45	3.4	3.5
Electron affinity	χ (eV)	-	4.5	4.5	4. 45	4.55	4.65
Relative permittivity	ε_r	-	13.6	13.6	10	9	9
VB DOS	N_v (cm^{-3})	-	4.12E18	2E18	1.5E19	9E18	9E18
CB DOS	N_c (cm^{-3})	-	7.96E17	2E18	2E18	4E18	4E18
Doping	N_A , N_D (cm^{-3})	-	8E15 (A)	5E16 (D)	5E17 (D)	1E18 (D)	1E20 (D)
Electron mobility	μ_n ($cm^2V^{-1}s^{-1}$)	-	100	1	100	100	100
Hole mobility	μ_p ($cm^2V^{-1}s^{-1}$)	-	25	1	25	25	25
Thermal velocity	v_{th} (cm/s)	-	1E7	1E7	1E7	1E7	1E7

Defect density	N_T (cm^{-3})	-	1E13	1E13	2E17	2E16	2E16
Electron capture cross-section	σ_e (cm^2)	-	5E-13	5 E-13	1E-13	1E-12	1E-12
Hole capture cross-section	σ^h (cm^2)	-	5E-15	5E-15	1E-13	1E-12	1E-12
Surface recombination velocity	S_b (cm/s)	variable	-	-	-	-	-
Work function	ϕ (eV)	variable	-	-	-	-	-

VB DOS: Density of states in the valence band, CB DOS: Density of states in the conduction band
A: Acceptor, D: Donor

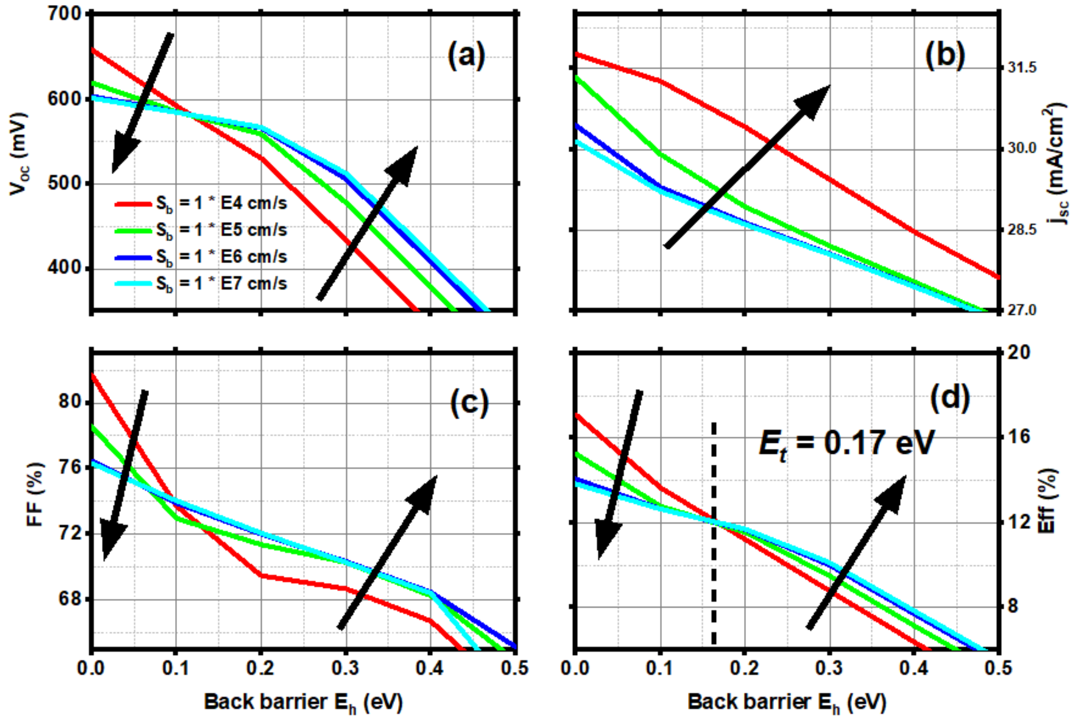

Figure S2. Simulated PV parameters for the solar cell structure of Table 3 dependent on the back potential barrier height E_h and recombination velocity S_b (red corresponds to S_b of 1*E4 cm/s, green to 1*E5 cm/s, blue to 1*E6 and cyan to 1*E7).

Using the settings listed in Table S3, the simulated PV parameters of full solar cells dependent on the back potential barrier E_h are obtained as shown in Figure S2. The arrows mark the direction of increasing recombination velocity S_b. The E_t marks the turning point of the conversion efficiency: when E_h is lower than E_t, a higher S_b decreases the efficiency, whilst for E_h higher than E_t, a higher S_b increases the *Eff*.

1. Manley, P., G. Yin, and M. Schmid, *A method for calculating the complex refractive index of inhomogeneous thin films*. Journal of Physics D: Applied Physics, 2014. **47**(20).